Int. J. Electrochem. Sci., 14 **(2019)** 2965 – 2983, doi: 10.20964/2019.03.79

International Journal of
ELECTROCHEMICAL
SCIENCE
www.electrochemsci.org

Solution Combustion Synthesis of Lithium Cobalt Oxide – Cathode Material for Lithium-Ion Batteries

VictorD. Zhuravlev[1], *Anna V. Shikhovtseva*[2], *Larisa.V. Ermakova*[1], *ElizavetaYu. Evshchik*[2,*], *Elena A. Sherstobitova*[3], *Dmitry V. Novikov*[4], *Olga V. Bushkova*[1,2,3], *Yuri A. Dobrovolsky*[2]

[1]Institute of Solid State Chemistry, Ural Branch of the Russian Academy of Sciences, Ekaterinburg 620990, Russia
[2]Institute of Problems of Chemical Physics, Russian Academy of Sciences, Chernogolovka 142432, Moscow Region, Russia
[3]M.N. Mikheev Institute of Metal Physics, Ural Branch of the Russian Academy of Sciences, Ekaterinburg 620990, Russia
[4]InenergyLlc, Moscow 115201, Russia
[*]E-mail: liza@icp.ac.ru

Received: 6 November 2018 / *Accepted:* 20 December 2018 / *Published:* 7 February 2019

A simple but novel solution combustion synthesis (SCS) technique suitable for $LiCoO_2$ scale production was developed. Citric acid was used together with glycine to slow down the combustion rate; cobalt(II) nitrate was partially replaced with cobalt(II) carbonate hydroxide to reduce the heating of the off-gases using the excess heat of the redox reaction. As a result, no open flame or eruption of the powder product out of the reactor was observed; the rapid SCS process occurring in the desired non-turbulent mode is suitable for scaling. The influence of the ratios cobalt(II) nitrate/cobalt(II) carbonate hydroxide and glycine/citric acid on the $LiCoO_2$ powder product properties was examined along with the influence of the post-combustion annealing conditions and pH of the precursor solution. The thus-obtained $LiCoO_2$ powders were characterised by X-ray diffraction, scanning electron microscopy and particle size distribution analysis. Testing of the electrochemical behaviour of the $LiCoO_2$ powders was performed in Li/$LiCoO_2$test cells having 1M LiDFOB in EC/DMC (1:1, wt.) as an electrolyte. The results confirmed the high electrochemical activity of the SCS-derived $LiCoO_2$powders; the best samples exhibited a discharge capacity ≥150 mAh g^{-1} and coulombic efficiency ≥99.5 % following 30 cycles at C/10 rate.

Keywords:lithium-ion batteries**;** lithium cobalt oxide; solution combustion synthesis.

1. INTRODUCTION

Although the present-day market for lithium-ion batteries (LIBs) is dominated by their use in portable electronic devices, more extensive applications are increasingly seen in electric vehicles

(EVs), hybrid EVs (HEVs) and smart grids [1-5]. From the first appearance of LIBs in 1991 and up to the present day, $LiCoO_2$still predominates in materials used for the positive electrodes of batteries, although new classes of electroactive compounds have been developed (and even commercialised) over the last three decades [1, 3, 6, 7]. The high operating voltage, sloping discharge curve, high coulombic efficiency of the charge and discharge processes, high specific capacity, cycling stability, acceptable self-discharge and simple industrial production of lithium cobalt oxide are all factors that explain its common usage in LIBs [7-10]. Pure $LiCoO_2$ has a reversible capacity of 135-150 mAh g^{-1} during the (de)lithiation process up to 4.3 V vs Li^0/Li^+ [4, 11-14]. $LiCoO_2$ coated with metal oxides, solid electrolytes, or polymers (see, for example, Refs. [15-18]) can be cycled up to the higher cut-off voltage of 4.5-4.7 V, which increases its discharge capacity up to 180-190 mAh g-1 [6, 11, 16]. In other words, coated $LiCoO_2$ can be used as a high-voltage cathode material, making it a material very promising for next-generation applications [6, 17]. Therefore, despite the high cost and toxicity of cobalt compounds, $LiCoO_2$ still retains its leading position and arouses unfailing research interest in both practical and scientific terms[10, 19].

The crystallinity and morphology of electroactive materials, which are essential factors in electrode performance [7, 9, 20], strongly depend on the starting materials and/or preparation method [9, 21]. To obtain a $LiCoO_2$ powder, various synthesis processes are used, including, solid-state synthesis [9, 22, 23], hydrothermal synthesis [24], the sol-gel method and its various modifications [15, 25-28], mechanochemical synthesis [29, 30], spray-pyrolysis [31-33], solution combustion synthesis [34-40] etc., these are briefly summarised in Ref. [9]. Over the past few decades, solution combustion synthesis (SCS) has emerged as an extensively-employed technique for the production of highly pure and well-crystallised powders of oxides, metals, alloys and sulphides used in many important applications [34-52]. The profound interest in combustion synthesis is mainly due to the simplicity and cost-effectiveness of the process, as well as the superior nature of the particulate properties of the products [46]. Moreover, controlling the combustion parameters allows the microstructure of the product to be easily varied [45].

In the recent review [39] and other works [45-52], solution combustion synthesis (SCS) was defined as a complex self-sustained redox process, which takes place in a homogeneous aqueous solution of starting materials, metal nitrates (oxidiser) and organic compounds having electron donor groups such as urea, glycine, citric acid, etc. In addition to supporting complex formation with metal cations and increasing salt solubility, these compounds serve as reducing agents (fuel) during a reaction. Following pre-heating to moderate temperatures (~150–200 °C), the reaction medium, in the form of a viscous liquid, self-ignites [52]. Further, owing to the high exothermicity of the system,the combustion temperature rapidly reaches ~1000°C and converts the precursor material into the desired complex oxide; the duration of the entire combustion process is usually a few minutes [39, 52]. The large number of gaseous products (H_2O, CO_2, N_2, etc.) results in a significant expansion of the solid product and a rapid decrease in temperature following the reaction, which gives the solid product its porous and finely dispersed properties. As emphasised in [39, 47], three features of SCS contribute to the unique properties of the synthesised product. Firstly, the initial aqueous solution allows all the raw materials to combine at themolecular level, thus permitting their homogeneous distribution and the precise formulation of the desired composition. Secondly, the high reaction temperatures (>900 °C) ensure the high purity and crystallinity of the product. This feature allows an additional step to be avoided – i.e., high-temperature product annealing, which typically follows the conventional sol-gel approach – for achieving the desired phase composition. (It must be noted that as-synthesised powders are nonetheless typically heat-treated in air to remove residual water and other volatile components thus improving the crystalline structure of the powders and influencing their microstructure [51]). Thirdly, the short process duration and formation of various gases during SCS inhibit particle size growth and favour the synthesis of nanosized powders having a high specific surface area [47]. Additional advantages of SCS are the absence of waste products (which excludes the need for their purification) and the possibility of regulating the composition of gaseous products, limiting them only to compounds contained in the air (nitrogen, water, carbon dioxide).

All of the above characteristics make SCS attractive for the synthesis of nanoscale (and not only) materials for a variety of applications, including LIBs [39]. Several works [34-37, 39] describe the solution combustion synthesis of $LiCoO_2$ with reactive solutions containing lithium and cobalt nitrates as an oxidiser and diformyl hydrazine [36], urea [34, 35], glycine [35], glucose [35] and starch [37] as a fuel. These solutions can ignite at a temperature as low as 250 °C [39], with the SCS process taking a few minutes. However, in order to obtain pure and well-crystallised $LiCoO_2$, a post-combustion annealing process lasting several hours was additionally used. In order to carry out a phase-pure, high-temperature modification of lithium cobalt oxide (HT-$LiCoO_2$),it was shown that the synthesis/annealing temperature should be excess of 600 °C, with the ideal layered α-$NaFeO_2$ structure (space group R-3m) having an ABCABC oxygen stacking [9, 34, 37, 39]. Products formed at lower temperatures consisted of both HT-$LiCoO_2$ and the low-temperature cubic form of lithium cobalt oxide (LT-$LiCoO_2$), which has poor cyclability. Post-combustion annealing also resulted in the aggregation of submicron particles of $LiCoO_2$ [34-37]. Positive electrodes prepared from combustion-derived $LiCoO_2$ exhibited substantial capacity of 110-136 $mA\cdot h\ g^{-1}$ and reasonably high-capacity retention over charge/discharge cycles [34, 36, 37]. In Ref. [38], three different carboxylic acids (citric, tartaric, and polyacrylic) were used together with cobalt and lithium nitrates for synthesis of $LiCoO_2$. The drying process resulted in the formation of foamy polymeric intermediates due to the generation of a huge number of gaseous molecules, but did not result in self-ignition and consequent transition into a self-sustained thermal process.

However, in addition to the aforementioned advantages, the SCS process has some unique features that complicate laboratory experiments and, more importantly, create barriers to the efficient industrial production of materials. The combustion synthesis in solutions of *d*-metal nitrates and commonly used organic fuels such as glycine, urea, hydrazine, etc. proceeds with high rate and open flame (see, for example, Ref. [35]). Multiple factors leading to an increased volume of the reaction mixture accompanying the SCS process cause potential problems in term of reactor overflow. In oxidative combustion mode and near the point of equivalence of the reducing agent and oxidiser, the reaction rate increases sharply and the flow of evolved gases can often eject all of the obtained powder from the reactor. Naturally, with increased mass of the material, these phenomena intensify. Moreover, in the presence of lithium nitrate, the process energy further increases. Another factor, often ignored by researchers, but which must be considered by producers, is the formation of toxic nitrogen dioxide when the reaction mixture is enriched with an oxidiser [34, 36].

In the present work, we developed a simple, novel technique suitable for scale application in the production of LIB materials by means of solution combustion synthesis of lithium cobalt oxide powder. Citric acid was used together with glycine to slow down the combustion rate; cobalt(II) nitrate was partly replaced with cobalt(II) carbonate hydroxide to reduce the heating of the off-gases and use the excess heat of the redox reaction. Investigations of the electrochemical performance of the $LiCoO_2$ powders in $Li/LiCoO_2$ test cells with 1M LiDFOB in EC / DMC (1:1, wt.) as electrolyte confirmed the high electrochemical activity of the obtained lithium cobalt oxide.

2. EXPERIMENTAL

2.1. Starting materials

For the combustion synthesis of $LiCoO_2$ and Co_3O_4 powders, cobalt(II) nitrate hexahydrate (99%) and cobalt(II) carbonate hydroxide hydrate $CoCO_3{\cdot}mCo(OH)_2{\cdot}nH_2O$ (with cobalt content of 55.5%) (both from Ural Chemical Reagents Plant, Russia) served as cobalt sources, lithium carbonate (UNICHIM (Russia), 99%) was used as a source of lithium; cobalt(II) nitrate also served as an oxidiser. Since cobalt salts are sufficiently hygroscopic, the cobalt content was determined prior to use by means of the standard analytical technique having an accuracy of ±0.1%. Citric acid hydrate $H_3C_6H_5O_7{\cdot}H_2O$ (Citrobel (Russia), 99.8%) and aminoacetic acid (glycine) $H_2N(CH_2)COOH$ (Kamhimkom (Russia), 98.5%) was used as fuel while double-distilled water served as a solvent for precursor solutions. The pH of the precursor solution was controlled with aqueous solution of ammonia (25%).

2.2. Synthesis

Table 1 presents the compositions of the aqueous precursor solutions for the combustion synthesis of the $LiCoO_2$ powder samples. An aluminium reactor with a volume of 2 dm^3 and a hot plate providing heating up to 300-350 °C were used for the combustion synthesis procedure.

Sample 1 was prepared using a two-step technique. Initially, submicron Co_3O_4 powder was prepared as follows. Appropriate amounts of fuels, glycine and citric acid (see Table 1) were added to cobalt nitrate solution having a cobalt concentration of 125 g l^{-1}. The solution was placed into the reactor and heated on a hot plate in contact with air up to the ignition temperature. The as-synthesised fine powder of cobalt oxides was then impregnated with an aqueous solution of lithium nitrate, obtained by dissolving a weighed amount of lithium carbonate in an equivalent amount of nitric acid (65%) under stirring. The resulting mixture of reagents, (Co_3O_4+CoO) powder and $LiNO_3$ solution, was dried and exposed to the two-stage annealing in a muffle furnace according to the conditions presented in Table 1 with intermediate grinding in a laboratory ball mill.

All other samples were prepared using a one-step technique according to which lithium salt is directly added to the precursor solutions.

In order to prepare Sample 2, a weighed amount of lithium carbonate was dissolved in an equivalent amount of nitric acid (65%) under stirring. After that, an appropriate amount of

$Co(NO_3)_2{\cdot}6H_2O$ was added to the solution, with the resulting concentration of the reagents becoming equivalent to 155.7 g l^{-1} of $LiCoO_2$. Next, the precursor solution was poured into the reactor and placed on a temperature-controlled hot plate; appropriate amounts of citric acid and glycine (see Table 1) were added to this solution with heating. Further, the acidity of the solution was reduced to pH 6-7 by addition of ammonia solution diluted at 1:1 ratio. With continuous heating, the solution was evaporated to form a gel; subsequently, during the process of its drying, a smooth, flameless SCS reaction started.

Table 1. Compositions of reaction mixtures for combustion synthesis of $LiCoO_2$ and details of post-combustion annealing.

		Precursor solution (reagent mixture)							Post-combustion annealing		
		Cobalt source			Lithium source						
Sample number	SCS procedure	Cobalt (II) nitrate, % *	Cobalt (II) carbonate hydroxide, % *	Cobalt (III) oxide, % *	Lithium carbonate, % *	Lithium nitrate, % *	Glycine/citric acid ratio [mol]	pH	Temperature, °C	Time, h	Intermediate milling
1**	Step 1	100	-	-	-	-	0.50/1.00	2	750	10	Yes
	Step 2	-	-	100	-	100	-	2	880 930	10 10	
2	One-step	100	-	-	100	-	0.41/1.00	6-7	900	10	No
3	One-step	70	30	-	100	-	0.80/1.00	2-3	850	10	No
4	One-step	50	50	-	100	-	0.80/1.00	2-3	850	10	No
5	One-step	70	30	-	100	-	0.50/1.00	2-3	850	10	No
6	One-step	50	50	-	100	-	0.31/1.04	2-3	700 850	10 10	Yes
7	One-step	50	50	-	100	-	0.31/1.04	2-3	700 850 900	10 10 10	Yes

* from stoichiometry

** two-step procedure was used: solution combustion synthesis of cobalt oxide powder (Step 1) followed by impregnation of as-synthesised powder with lithium nitrate solution, drying and annealing (Step 2)

The influences of the ratios between cobalt(II) nitrate and carbonate hydroxide, as well as between glycine and citric acid, on the combustion synthesis of $LiCoO_2$ was also evaluated along with the influence of post-combustion annealing conditions and pH of the precursor solution (Samples 2-7, Table 1). Glycine and citric acid were added into an aqueous solution of cobalt nitrate (82.5 g l^{-1} cobalt concentration) to prepare these samples, then the solution was heated up to 50-70 °C and the temperature maintained until the reagents were fully dissolved. Then, an appropriate amount of $CoCO_3{\cdot}mCo(OH)_2{\cdot}nH_2O$ (see Table 1) was added under stirring and heating, and, finally, a stoichiometric quantity of lithium carbonate was dissolved in the solution. The precursor solution was placed into the reactor and evaporated with heating to a degree of dehydration, at which a smooth transition to a mixed oxide began in the reaction mixture.

The as-synthesised powders (Samples 1-7) were homogenised and placed into alumina crucibles; Table 1 gives the regimes of the post-combustion annealing for each sample. For Samples 6 and 7, two- and three-stage thermal treatment with intermediate grinding was used.

The resulting powders obtained following post-combustion annealing were ground in the laboratory ball mill and analysed as described in Section 2.3.

2.3. Characterisation of powder samples

X-ray patterns of the $LiCoO_2$ powder samples prepared by SCS technique were obtained by Shimadzu XRD-7000 diffractometer (Cu $K\alpha_1$radiation, 2θ=10-80°) using the ICDD-ICPDS database. Structural parameters were refined by Rietveld technique using the Full prof software program [53]. The morphology of the $LiCoO_2$ powder samples was observed using a JEOL JSM 6390 LA scanning electron microscope. The surface area of the synthesised powders was determined using the BET adsorption method using low-temperature nitrogen adsorption (SORBI 4.1, Russia). Particle size distributions of the $LiCoO_2$ powders were identified by means of a laser particle size analyser (Horiba LA-950, Japan).

2.4. Electrochemical measurements

The electrochemical properties of the $LiCoO_2$ powder samples were assessed using two-electrode pouch cells. The composite electrodes were prepared by inkjet printing a homogenised mixture of the synthesised material, a conductive additive (acetylene black) and a binder (polyvinylidene fluoride dissolved in N-methyl-2-pyrrolidone) (weight ratio of solid components 80:10:10) onto an aluminium foil. The electrodes were compacted in a rolling mill and then dried under vacuum at 120° C for 12 h. The area of the prepared electrode was 2.25 cm^2. The active material loading of the electrode was about 4 mg cm^{-2}.

The electrochemical test cells Li │liquid electrolyte │$LiCoO_2$ were assembled within an argon-filled MBraun LAB Star glove box with moisture and oxygen levels less than 0.1 ppm. Lithium foil (99.9 %, Alfa Aesar) was used as a counter electrode. Celgard 2300 film was used as a separator. The electrolyte consisted of a solution of 1 M lithium difluoro(oxalato)borate (LiDFOB) in ethylene carbonate (EC) and dimethyl carbonate (DMC) (1:1 wt.); all components were supplied by Sigma Aldrich and used without further purification. The residual water content in the electrolyte solution did not exceed 30 ppm.

The galvanostatic charge/discharge cycling of the electrochemical cells was performed in the voltage range of 2.75–4.3 V vs. Li/Li^+ at *C*/10 rate using a P-20X80 multichannel potentiostat (Elins, Russia).

3. RESULTS AND DISCUSSION

3.1. Solution combustion synthesis of $LiCoO_2$

The present research is aimed at developing a simple, novel technique for solution combustion synthesis of the $LiCoO_2$ powder suitable for scale application in the production of LIB materials. Consequently, it was necessary to find ways to slow down the combustion rate of the precursor solution, in the order to be able to use the excess heat of the redox reactions and reduce the heating of the evolved gases. A successful outcome would allow us to prevent the appearance of an open flame, avoid the ejection of powder product from the reactor and to minimise stoichiometry disturbances due to lithium loss. An additional aim was to prevent the formation of toxic gaseous products such as CO, NO, NO2, etc. during the combustion process.

Different combustion conditions are realised as part of the SCS process depending on the value of fuel/oxidiser ratio (φ) [39, 51, 52]. $\varphi=1$ (stoichiometric conditions) means that the initial mixture of reagents does not require atmospheric oxygen for complete oxidation of the fuel, while $\varphi>1$ (<1) implies fuel-rich (lean) conditions. According to this prior circumstance, the combustion reaction can proceed in three different modes. With $\varphi<0.7$ (fuel-lean conditions), a comparatively slow and relatively low-temperature reaction mode occurs (smouldering combustion synthesis); with $0.7<\varphi<1.2$ (nearly stoichiometric conditions), rapid volume combustion synthesis (VCS) takes place at the highest temperature; with $1.2<\varphi<1.6$ (fuel-rich conditions), self-propagating high-temperature synthesis is realised. In turn, the characteristics of synthesised powders depend on the combustion mode. The crystalline structure of as-synthesised powders becomes more defined as φ increases: amorphous for $\varphi<0.7$and crystalline for $0.7<\varphi<1.6$. The specific surface area decreases slightly when $\varphi \rightarrow 1$, but substantially increases, however, for $\varphi >>1$ [39, 51, 52].

It follows from the above that the combustion synthesis parameters can be controlled in a goal-directed manner, allowing the process to be adapted to technological requirements.

It is not convenient to carry out combustion synthesis of $LiCoO_2$ under stoichiometric conditions, in VCS mode, because, at φ approaching 1, the burning rate – and, consequently, the flow velocity of evolved gases – is highest [45]. As a result, up to 80-100% of the fine powder product can be ejected from the reaction zone along with water vapour, carbon dioxide and nitrogen. In addition to this, the combustion intensity sharply increases in the presence of alkali metal nitrates in the precursor solution.

There are two main approaches to ensuring a more predictable solution combustion synthesis of $LiCoO_2$, both of which take place under fuel-rich conditions. The first is to carry out combustion synthesis with a large excess of a reducing agent (i.e., with $\varphi>>1$) (Approach1). Here, the combustion temperature decreases rapidly with increasing φ [45], and, as a result, the rate of the process is noticeably reduced. The second approach is to take a comparatively small excess of a reducing agent ($\varphi\geq1.2$) while using less-calorific fuel (Approach2).

Combustion synthesis under conditions of a large excess of fuel (Approach1) requires the influx of oxygen into the reaction zone for complete oxidation of the products. In reality, this does not occur due to the counter-flow of evolved gases from the reactor. As a result, toxic CO inevitably appears in the evolved gases; moreover, undesirable admixtures of unburned carbon and unoxidised residues of organic molecules are present in the solid products.

Therefore, the alternative approach to reducing the combustion intensity (Approach 2) was chosen for the synthesis of $LiCoO_2$ in this work. A mixture of citric acid and glycine was used as less-calorific fuel (see Table 1) with $\varphi \approx 1.2\text{-}1.8$. In addition, the expending of the heat of exothermic reaction for thermal decomposition of cobalt and lithium citrates obtained by dissolving cobalt and lithium carbonates in citric acid (see Section 2.2) allowed the energy of the combustion process to be reduced. The possibility that the metal carbonates partially reacted with aminoacetic acid (glycine), additionally forming its salts, cannot be excluded. Finally, lithium carbonate rather than lithium nitrate was used as a source of lithium since, if the solution contains lithium nitrate, the combustion reaction takes on an explosive character.

The following is an example of a general equation for $LiCoO_2$ combustion synthesis using mixed glycine/citric acid fuel:

$$Co(NO_3)_2 + CoCO_3{\cdot}Co(OH)_2 + Li_2CO_3 + H_3C_6H_5O_7 + 0.8H_2N(CH_2)COOH + 0.5O_2 \rightarrow 2LiCoO_2 + 1.4N_2 + 6.4CO_2 + 6.8H_2O \quad (1)$$

Here, it is worth noting that the participation of gaseous oxygen from air in the $LiCoO_2$ combustion synthesis reaction is required since cobalt changes its oxidation state from +2 to +3. Therefore, the as-synthesised powders are needed in post-combustion annealing in the air not only to remove residual water, unburned carbon, and organic fragments, but also to complete cobalt oxidation, as well as to complete the $LiCoO_2$ formation process and improve the product’s crystalline structure.

The typical combustion synthesis procedure included preparation of the precursor solution (as described in Section 2.2) and its pre-heating up to boiling point of water followed by constant-temperature treatment for about 0.5 h during which all free and partially-bound water was evaporated. Complex formation between metal ions (Co^{2+}, Li^{+}) and fuel molecules (glycine, citric acid) prevented salt precipitation during water evaporation and provided gelation of the solution; further dehydration caused its transformation into a xerogel. At a particular moment during its heating to moderate temperatures, self-ignition and propagation of a self-sustained, highly exothermic redox reaction occurred. The energy released during this process is sufficient to decompose the xerogel into a solid product and a mixture of gases. At the same time, no open flame or ejection of the powder product from the reactor was observed; the SCS process occurred in the desired non-turbulent mode. The whole procedure was rather brief, taking less than one hour. The resultant as-synthesised powders were then annealed in air under conditions presented in Table 1.

3.2. Characterisation of $LiCoO_2$preparedby combustion synthesis

The $LiCoO_2$ samples prepared by combustion synthesis were characterised by Rietveld refinement of powder X-ray data. A rhombohedral structure with space group *R-3m* of layered α-$NaFeO_2$-type served as a trial model for the Rietveld refinement of the x-ray diffraction data; lithium, cobalt and oxygen ions were located at Wyckoff positions of: 3a sites (0, 0, 0), 3b sites (0, 0, 0.5,) and 6c sites (0, 0, 0.25), respectively. Table 2 provides the results of Rietveld refinement. An asymmetric peak shape was observed in the XRD patterns of the Samples 1-5 (a typical XRD pattern is shown in

Fig. 1). The XRD patterns were satisfactorily fitted by two hexagonal phases (the structural type of α-$NaFeO_2$) with different *a* and *b* lattice parameter values. The first hexagonal phase had lattice parameters *a*=2.815±1Å, *c*=14.05±1 Å and a *c/a* ratio of 4.99 typical of stoichiometric $LiCoO_2$ [9]. The other phase, having smaller *a*(2.810±1 Å) and larger *c*(14.18±4 Å)values where *c/a*>5, was identified as a nonstoichiometric lithium cobalt oxide with Li/Co<1. In layered $LiCoO_2$, removal of lithium ions decreases the electrostatic shielding between O-Co-O sheets, which leads to an increase in the *c/a* ratio from 4.99 at full Li content to 5.13 in $Li_{0.5}CoO_2$ [9]. It is known, however, that Li_xCoO_2 with $x<1$ (Li+Co<O, presence of Li vacancies and Co^{4+} ions) can be obtained by electrochemical or chemical delithiation only; its formation by synthesis from precursors within Li/Co atomic ratio <1 and by heat treatment of $LiCoO_2$ at T>900 ºC is doubtful [9, 54]. Another kind of layered lithium cobalt oxide with Li/Co<1 is $Li_yCo_{2-y}O_2$ solid solution of CoO in $LiCoO_2$ (Li+Co=O, presence of Co^{2+} ions) [9, 55, 56, 57] with a*c/a* ratio >5 [55]. We conclude therefore that it is the $Li_yCo_{2-y}O_2$ phase that is present in Samples 1-5 along with the main phase of stoichiometric $LiCoO_2$ (Table 2). The presence of Co_3O_4 spinel phase impurity (Table 2) confirms lithium loss in Samples 1-5 during the synthesis procedure. Among these samples, the highest content of the $Li_yCo_{2-y}O_2$ solid solution (19 % (wt.)) was observed in Sample 1, while the highest content of the stoichiometric $LiCoO_2$ (93 % (wt.)) in Sample 2. When compare Table 1 and Table 2, it can be seen that Samples 3, 4 and 5 having identical conditions of post-combustion annealing (850 °C, 10 h) demonstrated nearly the same percentage of $Li_yCo_{2-y}O_2$ and Co_3O_4 impurities.

It is necessary to note that Samples 1-5 exhibited preferred (00*l*) plane orientation of crystallites revealed as an increased diffraction intensity from the (003) peak. The texture affects the relative intensity of XRD reflections and, as a consequence, decreases the accuracy of calculations of different phase percentage presented in Table 2 as well as occupancies of lithium and cobalt sites, thus decreasing refinement quality. Since XRD measurements for $LiCoO_2$ powders were performed taking conventional precautions against preferred orientation, it cannot be excluded that the agglomeration features of the crystallites can partially cause the observed texturing during post-combustion annealing.

Samples 6 and 7 exhibited single-phase stoichiometric $LiCoO_2$ (Table 2 and Fig. 2). One can conclude therefore that starting the post-combustion annealing process at a relatively low temperature of 700 °C (Table 1) provides efficient protection against unwanted lithium loss, which occurs precisely during post-combustion annealing. It is also worth noting that Samples 6 and 7 demonstrated a much lower degree of texture as compared with Samples 1-5.

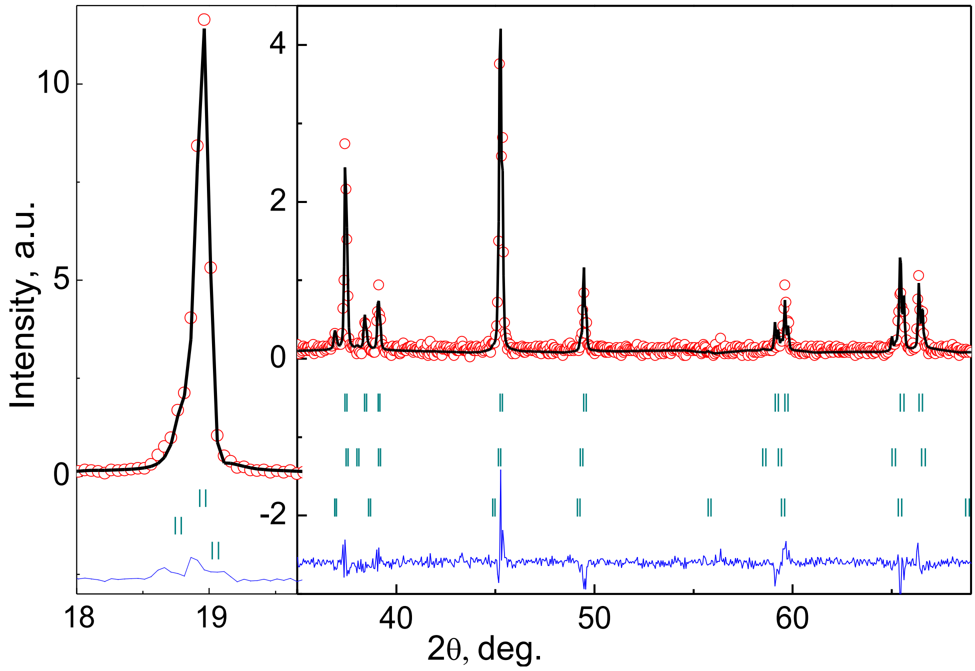

Figure 1. Powder X-ray diffraction pattern for Sample 1.The symbols represent experimental values of intensity while the lines represent the results of the Rietveld refinement. The difference curve between calculated and observed profiles is shown at the bottom. The upper row of vertical marks below the patterns refers to the Bragg peaks of the main $LiCoO_2$ phase, while the second row refers to the $Li_yCo_{2-y}O_2$ impurity phase and the lower row refers to the Co_3O_4 impurity phase.

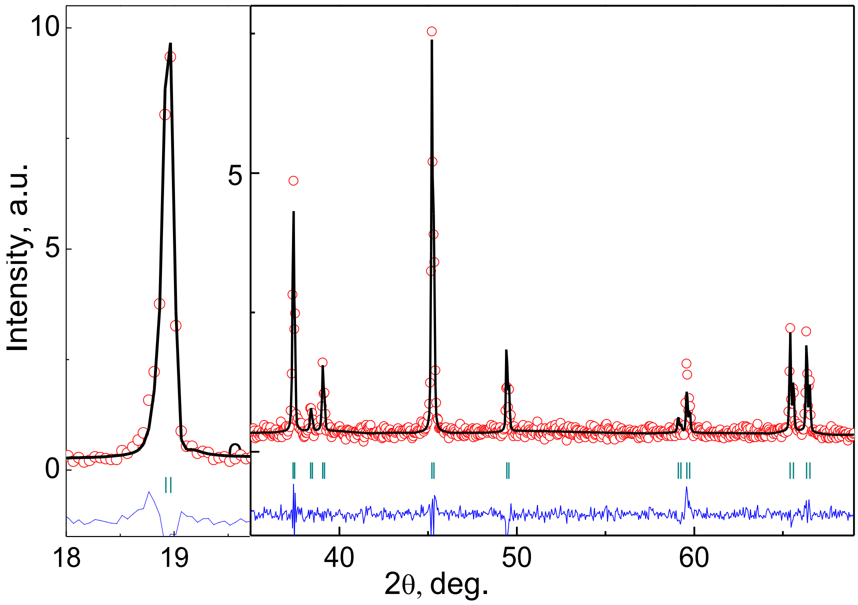

Figure 2. Powder X-ray diffraction pattern for Sample 7.The symbol represent experimental values of intensity while the lines represent the results of the Rietveld refinement. The difference curve between calculated and observed profiles is shown at the bottom. The row of vertical marks below the pattern refers to the Bragg peaks of the $LiCoO_2$ phase.

Table 2. Phase composition, cell parameters and morphology characterisation of the $LiCoO_2$ powder samples.

Sample number	XRD results						Morphology characterisation		
	Phase composition		S.G.	Cell parameters		*c/a*	BET		Particle size distribution
	Compound	Contents, % (wt.)		*a*, Å	*c*, Å		A_s, $m^2\ g^{-1}$	$\overline{D}$, μm	
1	$LiCoO_2$ $Li_yCo_{2-y}O_2$ Co_3O_4	78 ± 13 19 ± 9 3 ± 1	R-3m R-3m Fd-3m	2.8147(2) 2.8096(8) 8.0741(41)	14.0541(20) 14.1914(52)	4.99 5.05	1.1	3.2	Nearly uniform agglomeration with average particle size about 9 μm
2	$LiCoO_2$ $Li_yCo_{2-y}O_2$ Co_3O_4	93 ± 10 5.4 ± 0.4 1.9 ± 0.1	R-3m R-3m Fd-3m	2.8139(2) 2.8102(7) 8.0766(31)	14.0583(19) 14.2166(32)	5.00 5.06	1.1	3.1	Large coral-like agglomerates (up to ~100 μm) with a negligible fraction of small particles
3	$LiCoO_2$ $Li_yCo_{2-y}O_2$ Co_3O_4	83 ± 8 11 ± 4 6 ± 1	R-3m R-3m Fd-3m	2.8141(1) 2.8100(7) 8.0750(12)	14.0474(13) 14.1842(38)	4.99 5.05	2.2	1.6	Rounded agglomerates of 30-50 μm with a minor fraction of smaller particles (≤10 μm)
4	$LiCoO_2$ $Li_yCo_{2-y}O_2$ Co_3O_4	82 ± 7 8 ± 1 10 ± 1	R-3m R-3m Fd-3m	2.8142(1) 2.8107(9) 8.0751(18)	14.0486(14) 14.1656(55)	4.99 5.04	2.4	1.5	Wide particle size distribution, from ~2 μm to rounded agglomerates of about 40-50 μm
5	$LiCoO_2$ $Li_yCo_{2-y}O_2$ Co_3O_4	82 ± 1 9 ± 2 9±1	R-3m R-3m Fd-3m	2.8139(1) 2.8075(10) 8.0768(8)	14.0484(15) 14.1540(64)	4.99 5.04	1.8	2.0	Rounded agglomerates of 30-60 μm with a significant fraction of smaller particles (≤10 μm)
6	$LiCoO_2$	100	R-3m	2.8153(3)	14.0536(28)	4.99	1.9	1.9	Rounded agglomerates of 10-50 μm with a minor fraction of smaller particles (≤10 μm)
7	$LiCoO_2$	100	R-3m	2.8161(2)	14.0578(21)	4.99	0.9	3.9	Wide particle size distribution, from ~2 to ~80 μm

* by a laser particle size analysis

Figs. 3 and 4 demonstrate SEM images of all $LiCoO_2$ powder samples; both the magnification and the scale are specified in each micrograph. As can be seen, they are the same for all images so that the grain sizes and agglomeration can be compared directly. As evident from the micrographs, Samples 2-6 obtained by one-step SCS procedure (Table 1) demonstrate a rounded shape of crystallites with sufficiently close average size (from 0.5 to 1μm), but having a different agglomeration character (Fig. 4). It is also apparent from the SEM images for Samples 6 and 7 that the additional stage of thermal treatment (900 °C, 10 h for Sample 7) resulted in a remarkable increase (about two times) in the average crystallite size due to sintering. The highest values of crystallite sizes (>1.5 μm) and the most uniform agglomeration are intrinsic for Sample 1 (Fig. 3(a)) prepared using the two-step procedure. Sample 2 differs from other in terms of the very large coral-like agglomerates and the negligible fraction of small particles. Samples 3-5 are characterised by having nearly the same shape of crystallites and a wide distribution of agglomerate size. Table 2 summarises the results of SEM image analysis.

The specific surface area values for powder samples of $LiCoO_2$ are shown in Table 2 together with the average particle size values estimated by the relationship [34]:

$\overline{D}$=6/($\rho \cdot A_s$),

Where D is the average particle size, c is the theoretical density, and A_s is the specific surface area value obtained from the BET isotherms. As seen in Table 2, the surface area varies from 0.9 to 2.4 m^2 g^{-1} and the mean particle size$\overline{D}$from 1.5 to 3.9 μm depending on SCS conditions. The changes in these values for Samples 1-7 agree with the SEM analysis described above.

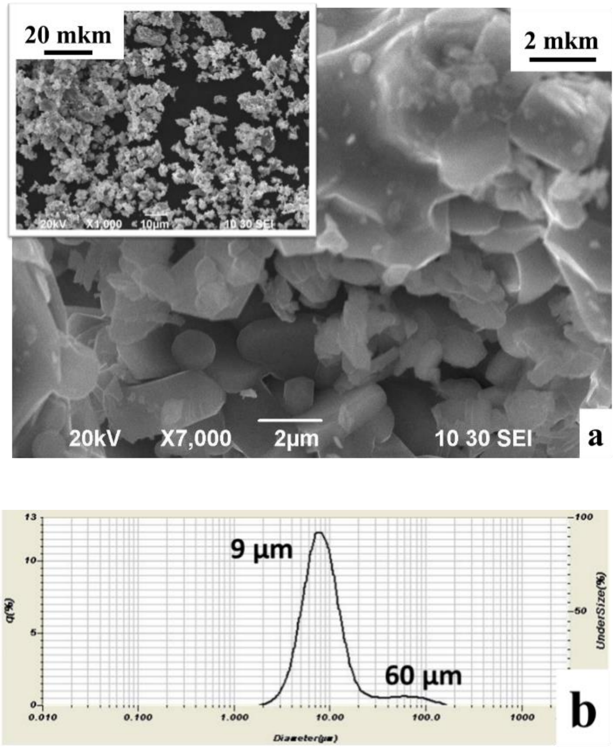

Figure 3.SEM image **(a)** and particle size distribution **(b)** for Sample 1 prepared by two-step SCS procedure

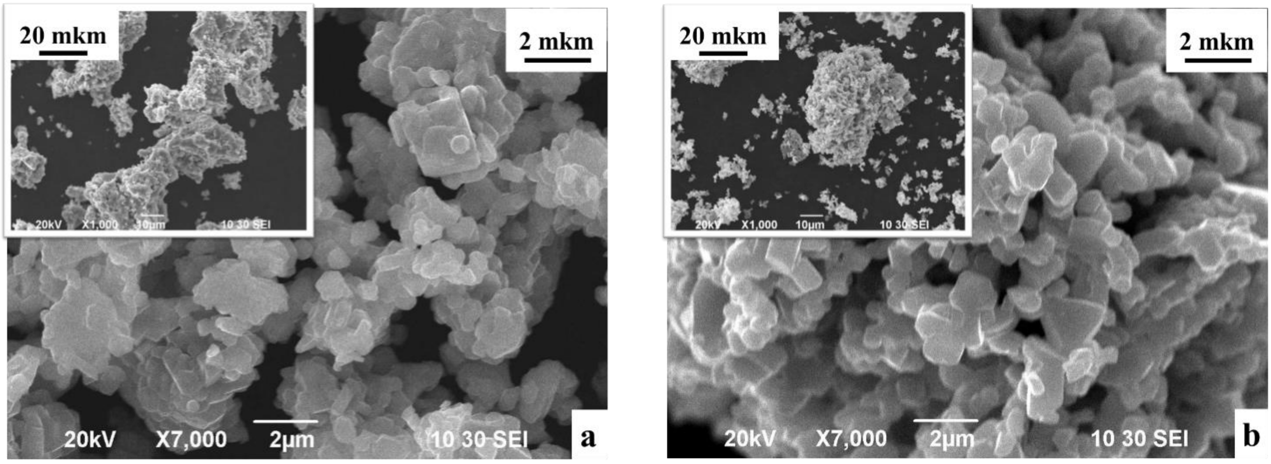

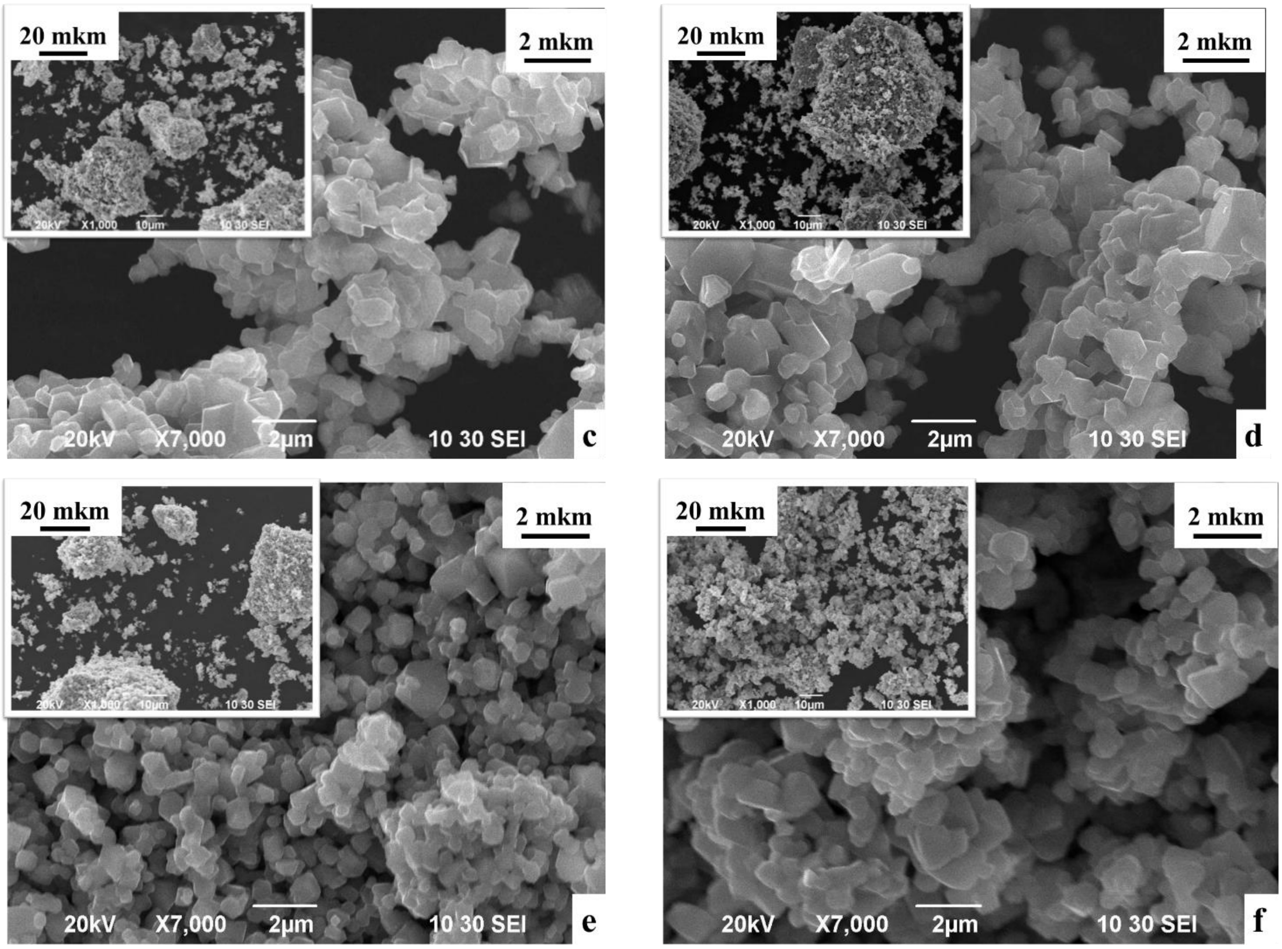

Figure 4.SEM images for the $LiCoO_2$ powder samples prepared by one-step SCS synthesis: Sample 2 **(a)**; Sample 3 **(b)**; Sample 4 **(c)**; Sample 5 **(d)**; Sample 6 **(e)**; Sample 7 **(f)**

The results of the characterisation of$LiCoO_2$ powders may be summarised as follows. The variation of the glycine/citric acid ratio (Samples 3 and 5) and the cobalt nitrate/cobalt carbonate ratio (Samples 3 and 4) had virtually no effect on the phase composition of the samples or the average crystallite size; their influence on the morphology morphology was primarily in terms of the agglomeration peculiarities. A perfect crystalline structure of stoichiometric $LiCoO_2$ was intrinsic for Sample 7; however, this powder had the widest particle size distribution and alarger crystallitesize. The most homogeneous particle size distribution with a sharp maximum at ~9 µm and very low maximum at ~60 µm characterised Sample 1, which had the highest$Li_yCo_{2-y}O_2$ admixture content.

3.2. Electrochemical measurements

Since $LiCoO_2$ is thermodynamically unstable in respect to $LiPF_6$ [58] and readily reacts with electrolyte solutions comprising this salt [59], LiDFOB served as an alternative [60] for electrochemical testing of lithium cobalt oxide powders. The charge and discharge performance of cells with $LiCoO_2$ powders prepared by SCS was examined in the range of 3.0-4.3 V at rate of C/10. Fig. 5 illustrates the cycle performance of Samples 1-7, while Table 3 summarises the cycling results.

It can be seen that Samples 1-3 exhibited the highest discharge capacity values (130-150 mAh g^{-1}) and that these values are equal to or higher than those presented in Refs. [34, 36, 37] for other combustion-derived $LiCoO_2$ powders. The discharge capacity of Samples 1-3 retains ~95.6, ~91.1 and ~94.3% of the original capacity after 25 cycles, respectively, whereas other samples keep less than 90% of the initial capacity. Moreover, Samples 1-3 had a coulombic efficiency of more than 99% (Table 3).

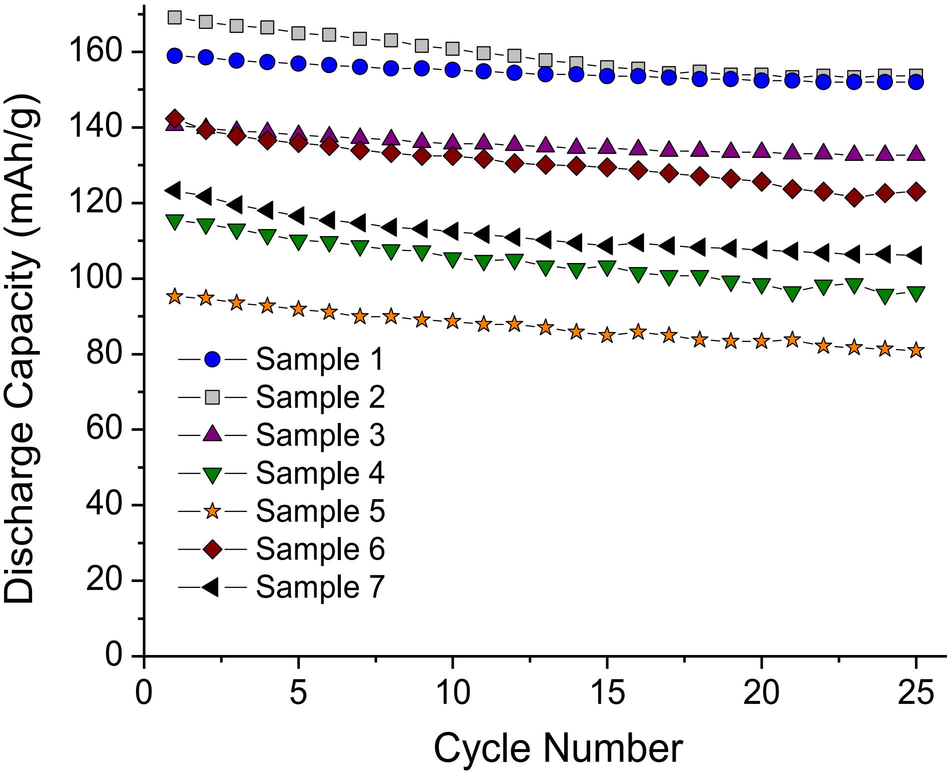

Figure 5. Discharge capacity as a function of cycle number for $LiCoO_2$ samples cycled between 3.0 and 4.3 V at the C/10 rate.

Fig. 6(a) displays the first charge-discharge curves for Samples 1-3 having the best electrochemical properties. The cells were initially charged from their rest potential up to 4.3 V and then discharged down to 3 V. The curves are quite similar to those reported previously (see, for example, Refs. [26,61-63]). The charge (Li extraction) and discharge (Li insertion) curves display a broad potential plateau at about 3.9 V vs Li/Li^+ and two small quasi-plateaus at about 4.1 and 4.2 V. These plateaus correspond to the peaks in the curves of differential capacity (dQ/dV) vs V shown in Fig. 6(b). According to literature data [9, 61, 62, 64, 65], the major peak at 3.9 V is associated with the first-order transition from $LiCoO_2$ to $Li_{0.8}CoO_2$; two less pronounced peaks at ~4.06 and ~4.17 V are related to phase transitions to the monoclinic structure and again to hexagonal.

Table 3. The cycle performance of $LiCoO_2$ powders in the range of 3.0–4.3 V at the C/10 rate.

Sample number	Discharge capacity, mA h g^{-1}		Coulombic efficiency for 25th cycle, %	Capacity retention for 25 cycles, %
	1st cycle	25th cycle		
1	159	152	99.7	95.6
2	169	154	99.5	91.1
3	141	133	99.4	94.3
4	116	96	98.5	82.8
5	95	81	99.0	85.3
6	142	123	85.0	86.6
7	123	106	90.0	86.2

The findings of this study demonstrate that Sample 6 comprising single-phase stoichiometric $LiCoO_2$ exhibited typical behaviour for the cycling of this material while lithium-deficient Samples 1-3 with admixtures of $Li_yCo_{2-y}O_2$ and Co_3O_4 had appreciably improved electrochemical properties. The significantly lower electrochemical properties of Sample 7 also comprising single-phase stoichiometric $LiCoO_2$ can be attributed to an increase in the average size of both crystallites and agglomerated particles, which reduces the electrochemical availability of the material. Poor electrochemical behaviour was observed for Samples 4 and 5, which are nearly identical to Sample 3 in their phase composition but markedly differ from it in terms of particle size distribution of agglomerates (Fig. 3 and Table 4). It cannot be ruled out that the reason for this consists in the out-washing of the smallest particles from the active mass. Among Samples 1 and 2 having the best electrochemical characteristics, Sample 2 seems to be preferable due to the simple one-step SCS procedure of its preparation suitable for scale application in the production of LIB materials.

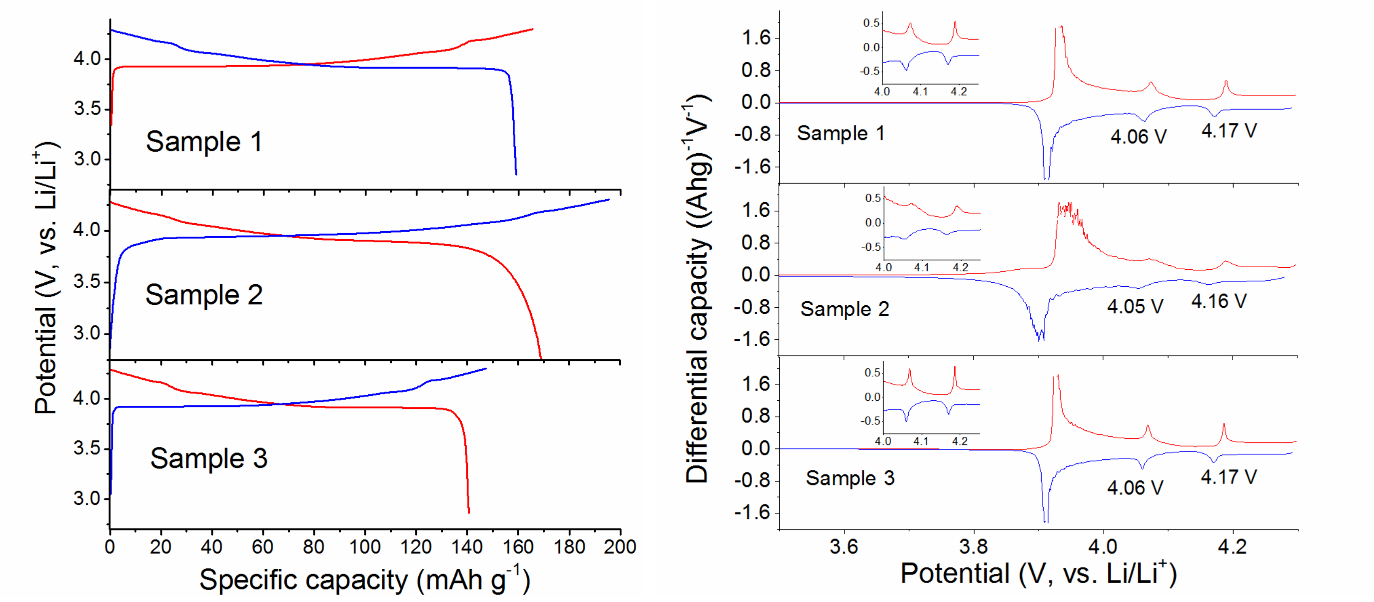

Figure 6. (a) First charge-discharge curves for $LiCoO_2$(Samples 1-3) cycled at the C/10 rate (b); differential capacity d*Q*/d*V* as a function of cell potential for first charge-discharge at the C/10 rate.

Table 4 summarises the electrochemical behaviour of positive electrodes based on $LiCoO_2$ powders obtained by different synthesis techniques (mechanical alloying of hydroxides, polymer pyrolysis, sol-gel, combustion synthesis and others). It can be seen that the values of the discharge capacity are within the range of 95-155 mAh/g, and that the electrochemical characteristics of the $LiCoO_2$ samples prepared by SCS in this work are comparable to or higher than those reported in the literature.

Table 4. Discharge capacity of $LiCoO_2$ obtained by various synthesis techniques.

Synthesis technique	Reagents	Voltage window, V	Discharge capacity, mA h g^{-1}	Cycle number	References
Hydrothermal synthesis	$Co(NO_3)_2$, LiOH, H_2O_2	2.7-4.25	120	22	[24]
	$Co(CH_3COO)_2$, $CO(NH_2)_2$ $(HO\text{-}CH_2CH_2)_3N$	3-4.3	150	100	[10]
Sol-gel synthesis	$LiOH{\cdot}H_2O$, $Co(OAc)_2{\cdot}4H_2O$, $HOOCCH(OH)(CH_2COOH)$	3.5-4.25 3.5-4.5	115	50	[66]
	$LiNO_3$, $Co(NO_3)_2{\cdot}6H_2O$, $C_6H_8O_7{\cdot}H_2O$, hydroxypropyl cellulose	3-4.2	154	25	[67]
	Co $(NO_3)_3{\cdot}6H_2O$, $LiNO_3$, citric acid	2.7-4.2	95	50	[68]
Sol-gel based electrospinning	Li (CH_3COO) $4H_2O$, $Co(CH_3COO)_2$	3-4.3	124	30	[69]
Solid-state synthesis	Li_2Co_3, $CoCO_3$	3.3-4.3	145	15	[70]
	Li_2Co_3, $CoCO_3$	3-4.2	118	25	[23]
Polymer pyrolysis	LiOH, Co $(NO_3)_2$, acrylic acid, $(NH_4)_2S_2O_8$	3.5-4.2	152	50	[71]
Mechanical alloying of hydroxides	$LiOH{\cdot}H_2O$, $Co(OH)_2$	2.7-4,25	125	30	[72]
Mechanochemical synthesis	Li_2CO_3, $CoCO_3$	3.3-4.3	160	100	[30]
Spray-pyrolysis	Li_2CO_3, $Co(CH_3COO)_2$, acetic acid	3-4.4	150	50	[32]
Soft chemistry	EDTA/Co/Li complex	2.7-4.2	167	30	[73]
Solution combustion synthesis	$LiNO_3$, $Co(NO_3)_2$, starch	3.5-4.3	110	30	[37]
	$Co(NO_3)_2$, Li_2CO_3, diformyl hydrazin	3-4.2	120	30	[36]
	$LiNO_3$, $Co(NO_3)_2$, urea	2.5-4.2	136	1	[34]
	$LiNO_3$, CoO, glycine, citric acid	2.75-4.3	152	25	This work
	Li_2CO_3, $Co(NO_3)_2$, glycine, citric acid	2.75-4.3	154	25	This work

4. CONCLUSION

A simple novel technique suitable for scale application in the production of LIB materials was developed for solution combustion synthesis of $LiCoO_2$ powder. Citric acid was used together with glycine to slow down the combustion rate; cobalt(II) nitrate was partly replaced with cobalt(II) carbonate hydroxide to reduce the heating of the off-gases and utilise the excess heat of the redox reaction. The findings demonstrated the possibility of the desired non-turbulent mode of the SCS process without any open flame, ejection of powder product from the reactor or toxic gas evolution. Variations in the ratio between cobalt(II) nitrate and carbonate hydroxide and between glycine and citric acid as well as pH of precursor solution influenced the agglomeration and particle size distribution rather than the average size of crystallites. The phase composition of the product was determined by post-combustion annealing conditions; starting at 700 °C, this provides effective protection against lithium loss and formation of lithium-deficient admixtures.

The best electrochemical properties, discharge capacity of 154 mAh g^{-1} and coulombic efficiency of 99.5 following 25 cycles at the C/10 rate were established for the sample obtained by one-step procedure from cobalt(II) nitrate and lithium carbonate as starting materials, glycine and citric acid as a fuel, pH=6-7 for the precursor solution, and post-combustion annealing at 900 °C (10 h). The electrochemical behaviour of thus obtained $LiCoO_2$is comparable with or better than those reported in the literature.

ACKNOWLEDGEMENTS

This work was supported by the Ural Branch of the Russian Academy of Sciences (Complex Program of Fundamental Research, grant No.18-10-3-32).

References

1. M. Hu, X. Pang, Z. Zhou, *J. Power Sources*, 237 (2013) 229.
2. C. M. Julien, A. Mauger, K. Zaghib, H. Groult, *Inorganics*,2 (2014) 132.
3. G.E. Blomgren, *J. of The Electrochem. Society*, 164 (2017) A5019.
4. K. Amine, R. Kanno, Y. Tzeng, *MRS Bull*, 39 (2014) 395.
5. C. Lim, B. Yan, H. Kang, Z. Song, W. Lee, V. D. Andrade, F. D. Carlo, L. Yin, Y. Kim, L. Zhu, *J. Power Sources*, 328 (2016) 46.
6. A. Zhou ,W. Wang , Q. Liu , Y. Wang, X. Yao , F. Qing, E. Li , T. Yang, L. Zhang, J. Li, Stable, *J. Power Sources*, 362 (2017) 131.
7. J. Geder, H.E. Hoster, A. Jossen, J. Garche, D.Y.W. Yu, *J. Power Sources*, 257 (2014) 286.
8. T. Lee, K. Cho, J. Oh, D. Shin, *J. Power Sources*, 174 (2007) 394.
9. E. Antolini, *Solid State Ionics*, 170 (2004) 159.
10. B. Wu, J. Wang, J. Li, W. Lin, H. Hu, F.Wang, S. Zhao, C. Gan, J. Zhao, *Electrochim. Acta*, 209 (2016) 315.
11. S. T. Myung, K. Amine, Y. Sun,*J. Power Sources*,283 (2015) 219.
12. L. Su, Y. Jing, Z. Zhou, *Nanoscale*, 3 (2011) 3967.
13. B. M.Winter, J. O. Besenhard, M. E. Spahr, P. Novak, *Adv. Mater.*, 10 (1998) 725.
14. Y.R. Zhu, T.E. Yi, *Ionics*, 22 (2016) 1759.
15. Q. Hao, H. Ma, Z. Ju, G. Li, X. Li, L. Xu, Y. Qian, *Electrochim. Acta*, 56 (2011) 9027.
16. J. Cao, G. Hu, Z. Peng, K. Du, Y. Cao, *J. Power Sources*, 281 (2015) 49.
17. J. Zhang, R. Gao, L. Sun, H. Zhang, Z. Hu, X. Liu, *Electrochim. Acta*, 209 (2016) 102.
18. C. Li, H.P. Zhang, L.J. Fu, H. Liu, Y.P. Wu,, E. Rahm, R. Holze, H.Q. Wu, *Electrochim. Acta*, 51 (2006) 3872.
19. E. Oz, S. Demirel, S. Altin, E. Altin, A. Bayri, S. Avci, *Electrochim. Acta*, 248 (2017) 449.
20. J. W. Fergus, *J. Power Sources*, 195 (2010) 939.
21. O.A. Brylev, O.A. Shlyakhtin, T.L. Kulova, A.M. Skundin, Yu.D. Tretyakov, *Solid State Ionics*, 156 (2003) 291.
22. E. Rossen, J.N. Reimers, J.R. Dahn,*Solid State Ionics*, 62 (1993) 53.
23. P. Periasamy,B.R.Babu,R. Thirunakaran,N.Kalaiselvi , T.P. Kumar,N.G. Renganathan, M.Raghavan,N.Muniyandi,*Bull. Mater.Sci.*, 23(2000) 345.
24. A.Burukhin,O.Brylev,P.Hany,B.R.Churagulov, *Solid State Ionics*, 151 (2002) 259.
25. S. Tao, Q.Wu, Z. Zhan, G. Meng,*Solid State Ionics*, 124 (1999) 53.
26. W.S. Yoon, K.B. Kim, *J. Power Sources*, 81–82 (1999) 517.
27. I.H. Oh, S.A. Hong, Y.K. Sun, *Mater. Sci.*, 32 (1997) 3177.
28. N. A. A. Aziz, T. K. Abdullah, A. A. Mohamad, *Ionics*, 24 (2018) 403.

29. N.V. Kosova, V.F. Anufrienko, T.V. Larina, A. Rougier, L. Aymard, J.M. Tarascon, *J. Solid State Chem.*, 165 (2002) 56.
30. F. Xu, H. Yan, J. Chen, M. He, Z. Zhang, C. Fan, G. Liu, *Ceram. Int.*, 43 (2017) 6494.
31. C. D. Snyders, E. E. Ferg, J. Schuelein, H. Loewe, *S. Afr. J. Chem.*, 69 (2016) 69 88.
32. K. Konstantinov, G.X. Wang, J. Yao, H.K. Liu, S.X. Dou, *J. Power Sources*, 119–121 (2003) 195.
33. Y. Li , C. Wan, Y. Wu, C. Jiang, Y. Zhu, *J. Power Sources*, 85 (2000) 294/
34. E.I. Santiago, A.V.C. Andrade, C.O. Paiva-Santos, L.O.S. Buloões, *Solid State Ionics*, 158 (2003) 91.
35. U. P. Kumar, A. S. Nesaraj, *J. Nano. Adv. Mat.*, 2 (2013) 75.
36. S. Rodrigues, N. Munichandraiah, A.K. Shukla, *J. Power Sources*, 102 (2001) 322.
37. P.Kalyani, N. Kalaiselvi, N. Muniyandi, *J. Power Sources*, 111 (2002) 232.
38. S. Vivekanandhan, M. Venkateswarlu, N. Satyanarayana, *Advanced Device Materials*, 1 (2016) 105.
39. A. Varma, A. S. Mukasyan, A. S. Rogachev,K. V. Manukyan,*Chem. Rev.*, 116 (2016) 14493.
40. V. D. Zhuravlev, O. V. Bushkova, A. V. Pachuev, K. V. Nefedova, *Electrochemical Energetics,*15 (*4*) (2015) 165 (in Russian).
41. V. D. Zhuravlev, V. G. Bamburov, L. V. Ermakova, N. I. Lobachevskaya, *Physics of Atomic Nuclei*, 78 (2015) 1389.
42. V.D. Zhuravlev, K.V. Nefedova, O.G. Reznitskikh, *Int. Scien. J. Altern. Ener. Ecol.*, 8 (2007) 22 (in Russian).
43. K.V. Nefedova, V.D.Zhuravlev, *Perspektivnyyematerialy*, (2011) 380 (in Russian).
44. S. M.Khaliullin, V. D., Zhuravlev, V. G Bamburov, *Int. J. Self-Propag. High-Temp. Synth*, 25 (2016) 139.
45. A.S. Mukasyan, P. Epstein , P. Dinka, *Proc. Combust. Inst.*, 31 (2007) 1789.
46. S. T. Aruna, A. S. Mukasyan, *Curr. Opin. Solid State Mater. Sci.*, 12 (2008) 44.
47. A. S. Mukasyan, P. Dinka, *Int. J. Self-Propag. High-Temp. Synth.*, 16 (2007) 23.
48. X. Wang, M. Qin , F. Fang, B. Jia , H. Wu , X. Qu , A. A. Volinsky, *J. Alloys Compd.*, 719 (2017) 288.
49. Q. Zhou, Y. Mou, X. Ma, L. Xue, Y. Yan, *J. Europ. Ceram. Soc.*, 34 (2014) 801.
50. G.Križan, J. Križan, R. Dominko, M. Gaberšček, *J. Power Sources*, 363 (2017) 218.
51. A.S. Mukasyan, C.Costello, K.P. Sherlock, D. Lafarga, A. Varma, *Separation and Purification Technology*, 25 (2001) 117.
52. K. Deshpande, A. Mukasyan, A.Varma, *J. Am. Ceram. Soc.*, 86 (2003) 1149.
53. J. Rodriguez-Carvajal, *Physica B*, 192 (1993) 55.
54. S. Levasseur, M. Ménétrier, E. Suard, C. Delmas, *Solid State Ionics*, 128 (2000) 11.
55. E. Antolini, M. Ferretti, *J. Solis State Chem.*, 117 (1995) 1.
56. E. Antolini, M. Daturi, M. Ferretti, *J. Mat. Sci. Lett.*, 15 (1996) 416.
57. E. Antolini, *Int. J. Inorg. Mat.*, 3 (2001) 721.
58. O. V. Bushkova, O. L. Andreev, N. N. Batalov, S. N. Shkerin, M. V. Kuznetsov, A. P. Tyutyunnik, O. V. Koryakova, E. H. Song, H. J. Chung, *J. Power Sources*, 157 (2006) 477.
59. O. V. Bushkova, O. L. Andreev, N. N. Batalov, S. N. Shkerin, M. V. Kuznetsov, A. P. Tyutyunnik, O. V. Koryakova, E. H. Song, H. J. Chung, *Electrochemical Energetics*, 5(*2*) (2005) 74 (in Russian).
60. O. V. Bushkova, T.V. Yaroslavtseva, Yu. A. Dobrovolsky, *Russ. J. Electrochem.*, 53 (2017) 677.
61. Y.M. Choi, S.I. Pyun, J.S. Bae, S.I. Moon, *J. Power Sources*, 56 (1995) 25.
62. J. N. Reimers, J. R. Dahn, *J. Electrochem. Soc.*, 139 (1992) 2091.
63. J. Xie, N. Imanishi, A. Hirano, M. Matsumura, Y. Takeda, O. Yamamoto, *Solid State Ionics*, 178 (2007) 1218.
64. G.G. Amatucci, J.M.Tarascon, L.C. Klein,*J. Electrochem. Soc.*, 143 (1996) 1114.
65. T. Ohzuku, A.Ueda, *J. Electrochem. Soc.*, 141 (1994) 2972.

66. X. L. Zeng, Y. Y. Huang, F. L. Luo, Y. B. He, D. G. Tong, *J. Sol-Gel Sci. Technol.*, 54 (2010) 139.
67. C. Zhu, C. Yang, W.D. Yang, C.Y. Hsieh, H.M. Ysai, Y.S. Chen, *J. Alloys. Comp.*, 496 (2010) 703.
68. L. Predoană, A. Barău, M. Zaharescu, H. Vassilchina, N. Velinova, B. Banov, A. Momchilov, *J.Eur. Ceram. Soc.*, 27 (2007) 1137.
69. Y. Ou, J. Wen, H. Xu, S. Xie, J. Li, *J. Phys. Chem. Solid.*, 74 (2013) 322.
70. Y. Gan, L. Zhang, Y. Wen, F. Wang, H. Su, *Particuology,* 6 (2008) 81.
71. L. Xiao, Y. Yang, Y. Zhao, X. Ai, H. Yang, Y. Cao, *J. Solid State Electrochem.*, 12 (2008) 149.
72. W.T. Jeong, K.S. Lee, *J. Power Sources*, 104 (2002) 195.
73. J. Liu, Z. Wen, Z. Gu, M. Wu, Z. Lin, *J. Electrochem. Soc.*, 149 (2002) A1405.